UNIVERSIDADE FEDERAL DE ALFENAS

JOSÉ EDSON CAETANO DA SILVA

IMPACT OF MITOCHONDRIAL UNCOUPLER ON OXIDATIVE STRESS AND ACUTE CHAGAS HEART DISEASE

ALFENAS/MG

2024

JOSÉ EDSON CAETANO DA SILVA

IMPACT OF MITOCHONDRIAL UNCOUPLER ON OXIDATIVE STRESS AND ACUTE CHAGAS HEART DISEASE

Dissertação apresentada ao Programa de Pós-Graduação em Ciências Biológicas da Universidade Federal de Alfenas (UNIFAL-MG) como requisito parcial para a obtenção do título de Mestre.
Área de concentração: Interação Patógeno-Hospedeiro

Orientador: Prof. Dr. Rômulo Dias Novaes
Coorientadora: Profa. Dra. Lívia de Figueiredo Diniz

ALFENAS/MG

2024

Sistema de Bibliotecas da Universidade Federal de Alfenas

Biblioteca Central

Caetano da Silva, José Edson .
Impact of mitochondrial uncoupler on oxidative stress and acute chagas heart disease / José Edson Caetano da Silva. - Alfenas, MG, 2024.
37 f. : il. -

Orientador(a): Rômulo Dias Novaes.
Dissertação (Mestrado em Ciências Biológicas) - Universidade Federal de Alfenas, Alfenas, MG, 2024.
Bibliografia.

1. Doença de Chagas. 2. Estresse Oxidativo. 3. Patologia Cardiovascular. 4. Miocardite. I. Dias Novaes, Rômulo, orient. II. Título.

Ficha catalográfica gerada no Sistema Eletrônico de Ficha Catalográfica do SIB/UNIFAL-MG

JOSÉ EDSON CAETANO DA SILVA

"IMPACT OF MITOCHONDRIAL UNCOUPLER ON OXIDATIVE STRESS AND ACUTE CHAGAS HEART DISEASE

O Presidente da banca examinadora abaixo assina a aprovação da Dissertação apresentada como parte dos requisitos para a obtenção do título de Mestre em Ciências Biológicas pela Universidade Federal de Alfenas. Área de concentração: Biologia Celular, Molecular e Estrutural das doenças agudas e crônicas.

Aprovada em: 29 de julho de 2024.

Prof. Dr. Rômulo
Dias Novaes
Presidente da
Banca
Examinadora
Instituição: Universidade Federal de Alfenas - UNIFAL-MG

Profa. Dra. Eliziária Cardoso dos Santos
Instituição: Universidade Federal dos Vales do Jequitinhonha e Mucuri - UFVJM

Profa. Dra. Evelise Aline Soares
Instituição: Universidade Federal de Alfenas - UNIFAL-MG

RESUMO

Ao desacoplar a fosforilação oxidativa, o 2,4-dinitrofenol (DNP) atenua a biossíntese de espécies reativas de oxigênio (EROs), que são conhecidas por agravar a miocardite Chagásica. Assim, o impacto da quimioterapia baseada em DNP na miocardite aguda induzida por *Trypanosoma cruzi* foi investigado. Camundongos C56BL/6 não infectados e infectados não tratados e tratados por gavagem com 100 mg/kg de benznidazol (Bz – tripanocida de referência), 5 e 10 mg/kg de DNP durante 20 dias foram investigados. 24 horas após o último tratamento, os animais foram eutanasiados e o sangue e coração foram coletados e analisados. A infecção por *T. cruzi* induziu acentuada parasitemia, inflamação sistêmica, carga parasitária cardíaca (DNA de *T. cruzi*), estresse oxidativo, infiltrado inflamatório e dano miocárdico microestrutural em camundongos não tratados. O tratamento com DNP agravou a parasitemia, o parasitismo cardíaco e os danos microestruturais, os quais foram atenuados por Bz. Assim como Bz, 10 mg/kg de DNP foi eficaz em atenuar a produção de EROs (totais, H_2O_2 e O_2^-), óxido nítrico (NO), lipídios (malondialdeído) e proteínas (proteínas carboniladas) oxidadas, TNF, IFN -γ, IL-10 e MCP-1/CCL2, anti-*T. cruzi* IgG, níveis de troponina I cardíaca, bem como infiltrado inflamatório e dano cardíaco em camundongos infectados. Em conjunto, nossos achados indicam que o DNP atua como fator de risco farmacológico, agravando a parasitemia, o parasitismo cardíaco e os danos microestruturais aos cardiomiócitos em camundongos infectados por *T. cruzi*. Estas respostas foram potencialmente relacionadas às propriedades antioxidantes e anti-inflamatórias do DNP na ausência de efeito tripanocida, o que favorece o parasitismo por enfraquecer os mecanismos antiparasitários pró-oxidantes e pró-inflamatórios do hospedeiro. Por outro lado, os efeitos cardioprotetores induzidos pelo Bz foram associados às respostas anti-inflamatórias e antiparasitárias eficazes, as quais protegem contra o parasitismo, o estresse oxidativo e os danos microestruturais cardíacos na doença de Chagas.

Palavras-chave: Doença de Chagas, estresse oxidativo, patologia cardiovascular, miocardite.

ABSTRACT

By uncoupling oxidative phosphorylation, 2,4-Dinitrophenol (DNP) attenuates reactive oxygen species (ROS) biosynthesis, which are known to aggravate infectious myocarditis in Chagas disease. Thus, the impact of DNP-based chemotherapy on *Trypanosoma cruzi*-induced acute myocarditis was investigated. C56BL/6 mice uninfected and infected untreated and treated with 100 mg/kg benznidazole (Bz, reference antiparasitic drug), 5 and 10 mg/kg DNP by gavagem during 20 days were investigated. Twenty-four hours after the last treatment, the animals were euthanized and the heart was collected for microstructural, immunological, biochemical and molecular analyses. *T. cruzi* infection induced marked parasitemia, systemic inflammation (e.g., cytokines and anti-*T. cruzi* IgG upregulation), cardiac parasite load (*T. cruzi* DNA), oxidative stress, inflammatory infiltrate and microstructural myocardial damage in untreated mice. DNP treatment aggravated parasitemia, heart parasitism and microstructural damage, which were markedly attenuated by Bz. Like thus drug, 10 mg/kg DNP was also effective in attenuating ROS (total ROS, H_2O_2 and O_2^-), nitric oxide (NO), lipid (malondialdehyde - MDA) and protein oxidation (protein carbonyl - PCn), TNF, IFN-γ, IL-10, and MCP-1/CCL2, anti-*T. cruzi* IgG, cardiac troponin I levels, as well as inflammatory infiltrate and cardiac damage in *T. cruzi*-infected mice. Taken together, our findings indicate that DNP acts as a pharmacological risk factor, aggravating parasitemia, heart parasitism and microstructural cardiomyocytes damage in *T. cruzi*-infected mice. These responses were potentially related to the antioxidant and anti-inflammatory properties of DNP in the absence of trypanocidal effect, which favors parasitism by weakening the host's pro-oxidant and pro-inflammatory antiparasitic mechanisms. Conversely, Bz-induced cardioprotective effects were associated with effective anti-inflammatory and antiparasitic responses, which protect against heart parasitism, oxidative stress and microstructural damage in Chagas disease.

Keywords: Chagas disease, cardiovascular pathology, myocarditis, oxidative stress.

SUMMARY

INTRODUCTION

Chagas disease (ChD) is a neglected parasitic affection recognized as the second most important cause of infectious cardiomyopathy worldwide according to Novaes *et al.* (2017), Nogueira *et al.* (2023), only behind COVID-19 (Omidi *et al.,* 2021). This disease is endemic in Latin America and is on the rise mainly in North America and Europe due to non-vector forms of *Trypanosoma cruzi* (etiological agent) contamination (e.g., vertical transmission, donation of infected tissues and organs, and laboratory accidents) (Echeverría *et al.,* 2020; Who, 2023). Chagas disease is closely related to poverty and limited access to health services (Guhl, Ramírez, 2021; Who, 2023). Accordingly, most cases of infection are diagnosed late, and are almost invariably associated with serious electromechanical cardiovascular complications (Echeverría *et al.,* 2020; Suárez *et al.,* 2022).

Chagas heart disease is the most disabling and deadly manifestation of *T. cruzi* infection according to Novaes *et al.* (2017), Nogueira *et al.* (2023). This is a complex condition that courses with cardiomyocytolysis, autonomic denervation, persistent inflammation, autoimmune damage, and oxidative stress determined by free radicals upregulation (e.g., $OH^{\bullet-}$, $O_2^{\bullet-}$, and $ONOO^{\bullet-}$) and antioxidants insufficiency (e.g., enzymatic and non-enzymatic effectors) (Gupta *et al.,* 2009; Santos *et al.,* 2019). Although Chagas cardiomyopathy (CC) is multifactorial, redox imbalance plays a prominent role in its pathogenesis, being mediated by disturbances in mitochondrial complexes I and III in *T. cruzi*-infected cardiomyocytes, nitric oxide synthase (iNOS) and NADPH oxidase II upregulation in activated leukocytes (e.g., respiratory burst) (Wen; Garg, 2004, 2008; Gupta *et al.,* 2009). Despite the antiparasitic purpose, the nonspecific nature of these pro-oxidant reactions determines extensive microstructural and molecular cardiac damage, worsening myocarditis (Paiva *et al.,* 2018; Santos et al., 2019). As the host cannot naturally eliminate the parasite, inflammation and oxidative stress persist and feed on each other, determining progressive morphofunctional cardiac degeneration, heart failure and eventually death (Paiva *et al.,* 2018; Sánchez-Villamil *et al.,* 2020; Torrico *et al.,* 2021).

Classically, it has been proposed that *T. cruzi* is highly sensitive to oxidative stress (Igoillo-Esteve *et al.,* 2007). Accordingly, some studies suggest that pro-oxidant effectors (e.g., NO, HClO and H_2O_2) participate in *T. cruzi* elimination and replicative control by the host's cellular-based immune defenses (Machado *et al.,* 2012; Paiva; Bozza, 2014). However, divergent evidence indicate that the oxidative environment favors infection, becoming a stimulus for parasite growth in the acute phase, as well as for cardiomyopathy onset and

progression in the chronic phase of ChD (Goes *et al.,* 2016). Despite this controversy, previous studies indicate that modulation of redox metabolism may be relevant to attenuating pathological outcomes associated with *T. cruzi* infection, including CC (Novaes *et al.,* 2016, 2017; Sánchez-Villamil *et al.,* 2020). In this sense, antioxidant therapy with vitamins (egg., C and E) according to Tieghi *et al.* (2017), resveratrol as described by Vilar-Pereira *et al.* (2016) and curcumin second study by Novaes *et al.* (2016) exerted marked myoprotective and/or cardioprotective effects, attenuating parasitism, molecular oxidation (e.g., lipid and protein), and myocarditis in *T. cruzi*-infected mice (Vilar-Pereira *et al.,* 2016; Sánchez-Villamil *et al.,* 2020).

Currently, antioxidant therapy applied to Chagas disease is mainly focused on free radical scavengers (Novaes *et al.,* 2017; Sánchez-Villamil *et al.,* 2020; Maldonado *et al.,* 2021). However, the neutralization of these molecules only occurs after their production, enabling the prior activation of signaling pathways linked to cell parasitism. This characteristic could partially explain the limited therapeutic effectiveness of some antioxidants, including vitamins C and E (Gusmão *et al.,* 2012*;* Marim *et al.,* 2012; Novaes *et al.,* 2017). Although *T. cruzi*-induced mitochondrial dysfunction is the main source of pro-oxidant effectors in cardiomyocytes, direct mitochondrial inhibition of free radical biosynthesis has been overlooked. Thus, the availability of mitochondrial uncouplers represent a valuable opportunity in the search for more effective cytoprotective and cardioprotective redox modulators according to Geisler, (2019) in ChD as described by Sánchez-Villamil *et al.* (2020), Maldonado *et al.* (2021).

2,4-dinitrophenol (DNP) is a classic mitochondrial uncoupler, which acts through the dissociation of electron transport in the respiratory chain (Geisler, 2019). In this process, DNP attenuates reactive oxygen-derived species (ROS) biosynthesis and prevents oxidative stress (Geisler, 2019). Accordingly, DNP may be more efficient in preventing oxidative stress compared to antioxidants that act in the cytosol, avoiding excessive ROS production and the exhaustion of endogenous antioxidant effectors (Nasab *et al.,* 2004; Geisler, 2019). Considering the mechanism of action of DNP, this drug may be relevant in modulating the oxidative stress invariably triggered by *T. cruzi* infection, having a potential impact on ChD severity and progression. Thus, the impact of DNP-based chemotherapy on *Trypanosoma cruzi*-induced acute myocarditis was investigated. In addition to reactive oxygen species (ROS) production, protein and lipid oxidation, immunological, parasitological and microstructural cardiac outcomes associated to DNP treatment were evaluated and compared to Bz-based reference chemotherapy.

2 METHODOLOGY

2.1 Experimental conditions and groups

Female C57BL/6 mice with 8 weeks-old and 33.95±3.77g were kept in facilities with temperature (20 ± 2ºC), air humidity (60-70%) and photoperiod (12h/12h light/dark) controlled (Sequetto *et al.,* 2014). Water and rodent chow were provided *ad libitum*. The sample size in each experimental group was determined as previously reported (Nogueira *et al.,* 2023). Briefly, a 50% probability (P=1/2) to increase or decrease the variables of interest was admitted. Considering 95% confidence and 5% significance level (α=0.05), the minimal significant number of animals used was $P=(1/2)^{events}$; so, if n=5, $P=(1/2)^5$ or P=0.03; thus, P<0.05. From this result, we admitted an equivalent probability of sample loss due to *T. cruzi* infection. Thus, the final sample size was established in 10 animals per group. The animals were numerically codified and randomized into 5 groups using the random function of the Excel software, as follows: UU= Uninfected untreated, INF= Infected untreated, Bz= Infected treated with 100 mg/kg benznidazole (reference trypanocidal drug), DNP1= Infected treated with 5 mg/kg DNP, DNP2= Infected treated with 10 mg/kg DNP.

2.2 *Trypanosoma cruzi* infection and treatments

Mice were intraperitoneally inoculated with 2000 trypomastigotes of *T. cruzi* isolated from the peripheral blood of infected animals (Mendonça *et al.,* 2020). The inoculum size was obtained by serial dilution of infected blood in 0.9% NaCl solution as previously reported (Felizardo *et al.,* 2018). The parasite Y strain (DTU II) was used due to its high infectivity, pathogenicity and partial resistance to Bz (Diniz *et al.,* 2018). *T. cruzi* infection was microscopically confirmed 5 days after *T. cruzi* inoculation by trypomastigotes identification in 5µl blood samples, as previously reported (Novaes *et al.,* 2017). The infection was allowed to develop for 15 days to avoid excessive and unnecessary animal debility, according to ethical recommendations (Felizardo *et al.,* 2018). DNP and Bz were suspended in distilled water and administered by gavagem after confirm the infection (5 days post-*T. cruzi* inoculation). The animals were treated with 100 µL DNP at 5 and 10 mg/kg considering the high intestinal absorption, hepatic and muscular biodistribution (Geisler, 2019). This concentrations correspond to a human equivalent dose (HED) of 22.5-45.0 mg/day (Geisler, 2019). These doses were effective in modulating cardiac energy metabolism

(Vercesi; Focesi, 1973), in addition to increasing thermogenesis in mice in response to respiratory chain uncoupling (Bhattacharjee *et al.,* 2018).

Benznidazole was administered at 100 mg/kg, which corresponds to 7 mg/kg/day for human adults based on body surface area as described by Mazzeti *et al.* (2018), and is the reference trypanocidal dose in mice (Diniz *et al.,* 2018; Gonçalves-Santos *et al.,* 2019). Uninfected and infected untreated (receiving water by gavage) mice were used as controls (Novaes *et al.,* 2017). Treatments preparation and administration were conducted by two independent researchers, which were blinded to the intervention groups. The experimental outcomes were also blindly evaluated in relation to the intervention groups. The Institutional Ethics Committee for Animals Research approved this study (protocol number 013/2016).

2.3 Blood and heart parasitism assay

Blood parasitism was microscopically analyzed daily from a classical parasitological protocol (Brener, 1962). Briefly, peripheral blood aliquots (5µl) were collected from the animals' tail, distributed in histological slides and spread under 22mm×22 mm glass coverslips. The blood was microscopically observed using ×40 objective lens and ×10 ocular lens (×400 magnification). Parasites were randomly quantified in 50 non-coincident microscopic fields, and the average parasitemia was quantified (FELIZARDO et al., 2018). Twenty-four hours after the last treatment and/or parasitemia analysis, the animals were anesthetized (300 mg/kg ketamine and 30 mg/kg xylazine) and euthanized by exsanguination. Heart and blood were collected and used for biochemical, immunological, molecular, and microstructural analyses.

Heart parasitism was determined in heart samples by real time quantitative PCR (qPCR) as previously described (Santos *et al.,* 2015). Briefly, heart samples were homogenized and genomic DNA was extracted using a commercial kit following the manufacturer’s instructions (Promega, São Paulo SP, Brazil). DNA samples were adjusted to 25 ng/µL and PCR reactions were standardized at 10 µL volume containing 50 ng DNA, 5 µL SYBR Green (Applied Biosystems, CA, USA), 0.50 µM TNF primers or 0.35 µM 195-bp *T. cruzi* DNA primers (Table 1). From 96-wells plate, standard curve based on negative controls with mice-specific and *T. cruzi*-specific primers without DNA and with DNA from uninfected mice was obtained (Santos *et al.,* 2015). Parasite load (PL) based on *T. cruzi* DNA levels was normalized considering the results obtained for TNF as follows: PL = (mean *T. cruzi* DNA/mean TNF DNA) × 1000; where the constant 1000 is the expected TNF

concentration in 30 mg heart samples. Amplification efficiency (*E*) was calculated as (*E*) = $10^{-1/slope}$ (StepOne Software, ThermoFisher, MA, USA) (Stordeur *et al.,* 2002).

2.4 Reactive oxygen species and nitric oxide assay

Heart samples were frozen in liquid nitrogen (-196°C), pulverized in a crucible and treated with lysis buffer (2% Triton X-100, 50 mM Tris [pH 7.5], 40 mM HEPES, and 1 mM EDTA supplemented with 1 mM phenylmethanesulfonyl fluoride). The homogenate was sonicated for 1 min on ice and centrifuged at 8000×*g* for 10 min and 4ºC, the supernatant was collected (150 µl) and used in total ROS assay. General pro-oxidants were quantified using the CM-H2DCFDA probe (Waltham, Massachusetts, USA), a broad-spectrum ROS indicator that emit fluorescence upon oxidation. ROS were quantified from fluorescence spectroscopy using a 96-wells microplate reader (Varioskan, ThermoFisher Scientific, Waltham, Massachusetts, USA). Briefly, 80 µL heart supernatant and lysis buffer (control) were distributed in each well and were treated with 10 µM CM-H2DCFDA prepared in PBS. The plates were immediately read at 37°C for monitoring CM-H2DCFDA oxidization rate, with respective excitation/emission at 485nm/520 nm, as previously reported (Dias *et al.,* 2017). ROS levels were expressed as relative fluorescence units (RFU)/min.

Nitric oxide was estimated from nitrite/nitrate (NO_2^-/NO_3^-) quantification in heart homogenate as previously reported (Mendonça *et al.,* 2020). For this, a 96-well biochemical kit was used according to the manufacturer's instructions (Nitric Oxide Assay [EMNSO], ThermoFisher Scientific, Waltham, MA, USA). This is a colorimetric assay based on the Griess reaction, in which the enzyme nitrate reductase is used to convert nitrate in nitrite. Thus, nitrite is spectrophotometrically measured as a colored azo dye product at 540 nm (Anthos Zenyth 200; Biochrom, Cambridge, UK). The assay sensitivity was 0.222 µM and 0.625 µM for nitrite and nitrate, respectively.

2.5 Lipid oxidation assay

Lipid oxidation was estimated from malondialdehyde (MDA) levels in heart samples. For such, MDA was quantified by high-performance liquid chromatography (HPLC), as previously reported (Brown; Kelly, 1996). Briefly, heart samples were homogenized in lysis buffer (2% Triton X-100, 50 mMTris [pH 7.5], 40 mM HEPES, and 1 mM EDTA supplemented with 1 mM phenylmethanesulfonyl fluoride) at 4 ºC for 1 min, and centrifuged

for 15 min at 13000 ×*g*. The supernatant was treated with acetonitrile to precipitate proteins, filtered through a 0.2 pm filter and separated on a 250 mm × 4.6 mm i.d. VC-ODS RP18 column with 25 mM phosphate buffer (pH 6.5). Methanol was used as the mobile phase and a 0.8 mL min^{-1} flow rate. Fluorometric detection was performed at 532nm/553 nm excitation/emission using a RF-10AXL detector coupled to the HPLC system (Shimadzu Scientific Instruments, Kyoto, Japan) to ensure the sensitivity for low concentrations of the MDA-TBA2 adduct. Tetraethoxypropane was processed in the same way and was applied to calibrate MDA-TBA peak (Brown; Kelly, 1996).

2.6 Protein oxidation assay

Protein carbonyl (PCN) content was concurrently measured using a modified colorimetric biochemical assay based on 2,4-dinitrophenylhydrazine (DNPH) (Mesquita *et al.,* 2014). Briefly, pellets obtained after centrifuging the heart homogenates were incubated for 15 min with 0.4 mL of 10 mM 2,4-dinitrophenylhydrazine (DNPH) prepared in 0.5 M H_3PO_4 solution. Then, 200 µL NaOH (6 M) was added and incubated for 10 min. The reaction for oxidized proteins involved derivatization of the carbonyl group with DNPH, which generates a stable 2,4-dinitrophenyl (DNP) hydrazone metabolite. The reaction was read by spectrophotometry at 450 nm (Anthos Zenyth 200, Biochrom, Cambridge, UK).

2.7 Heart histopathology and histomorphometry

Heart fragments were fixed for 24h with 4% paraformaldehyde prepared in 0.1 M sodium phosphate buffer (pH 7.2) (Sequetto *et al.,* 2014). Then, fragments were embedded in plastic resin (glycol methacrylate) and 3-µm thick heart sections were obtained using glass knives coupled in a rotary microtome (Leica Biosystems, Wetzlar, Germany). Six heart sections were obtained in semi-series for each animal, so that one in each 30 sections were collected to avoid analyzing the same histological area. The sections were stained at 60 ºC with hematoxylin and eosin according to Mendonça *et al.* (2020) and only hematoxylin according to Ivanova *et al.* (2021). Ten random non-coincident microscopic images were obtained for each animal by bright field microscopy at ×400 magnification (Axioscope A1; Carl Zeiss, Germany). Heart pathological microstructural remodeling was analyzed considering: (i) parenchyma and stroma distribution, (ii) tissue necrosis, (iii) inflammatory infiltrate, (iv) myocyte hypertrophy or atrophy, (v) blood vessels distribution, and (vi) *T. cruzi*

nests distribution (Rodrigues *et al.,* 2017). These abnormalities were globally expressed using the polygonal method, which is based on a field diagram organized in four domains: (-) normal, (- - +) mild, (+ +) moderate or (+ + +) severe damage (Felizardo *et al.,* 2018). Interstitial cellularity and inflammatory infiltrate were quantified from the Image-Pro Plus software (Media Cybernetics Inc., Silver Spring, MD, USA) (Novaes *et al.,* 2018). A pathologist blinded to the intervention groups performed all morphological analysis.

2.8 Macrophages and neutrophils heart influx

Macrophages accumulation/activation was estimated from N-acetyl-β-D-glucosaminidase (NAG) activity in heart samples as previously reported (Mendonça *et al.,* 2020). N-acetyl-β-D-glucosaminidase is a lysosomal enzyme intensely expressed by activated macrophages. Enzyme activity was measured in fresh heart samples, which were homogenized in sodium phosphate buffer supplemented with protease inhibitor cocktail (Sigma-Aldrich, St. Louis, MO, USA) and centrifuged at 3000×*g* for 15 min (4 °C). The heart supernatant was collected and analyzed using a commercial biochemical colorimetric kit following the manufacturer's instructions (Abcam, Cambridge, UK). This method is based on a synthetic p-nitrophenol derivative (R-*p*NP) as NAG substrate, whose reaction product (pNP) can be detected by spectrophotometry at 400 nm (Mendonça *et al.,* 2020).

Neutrophils influx was estimated from myeloperoxidase (MPO) activity in heart samples as previously reported (Mendonça *et al.,* 2020). After centrifuging the heart homogenate, the corresponding pellets were weighed, homogenized in pH 4.7 buffer (0.02 M Na_3PO_4, 0.015 M Na_2-EDTA, and 0.1 M NaCl), and centrifuged for 10 min at 12,000×*g* (4 °C). The pellets were resuspended in 0.05 M sodium phosphate buffer containing 0.5% hexa-1,6-*bis*-decyltrimethylammonium bromide. Myeloperoxidase activity was measured by spectrophotometry at 450 nm (Anthos Zenyth 200, Biochrom, Cambridge, UK), using 1.6 mM 3,3′-5,5′-tetramethylbenzidine dissolved in dimethyl sulfoxide and 0.3 mM H_2O_2 prepared in pH 6.0 sodium phosphate buffer.

2.9 Cardiac Troponin I Assay

Cardiac troponin I (cTnI) circulating levels were quantified in serum samples as a marker of heart/cardiomyocytes damage (Gonçalves-Santos *et al.,* 2023; Nogueira *et al.,*

2023). For this, blood samples (300 µL) collected during euthanasia were centrifuged (12,000×*g*, 15 min and 4ªC) in the presence of protease inhibitor cocktail (Sigma-Aldrich, San Luis, MO, USA). The serum was collected and cTnI levels were quantified from an enzyme-linked immunosorbent assay (ELISA) kit following the manufacturer's instructions (MyBioSource, San Diego, CA, USA). cTnI was quantified by spectrophotometry at 450 nm by using a 96-wells microplate reader (Anthos Zenyth 200, Biochrom, Cambridge, UK).

2.10 Cytokines immunoassay

The cytokines interferon gamma (IFN-γ), tumor necrosis factor (TNF), interleukin 10 (IL-10), and the chemokine monocyte chemoattractant protein-1 (MCP-1/CCL2) were quantified in the same heart homogenate obtained in the NAG assay. All cytokines were quantified using a commercial cytometric bead array (CBA) mouse kit, according to the manufacturer's instructions (BD Biosciences, San Diego, CA, USA). Standard curves ranging from 20-5000 pg/mL were constructed from recombinant cytokines. The lower limit of detection in this assay was 2.5-52.7 pg/mL. Data were collected and analyzed using the FACSVerse flow cytometer and FCAP software (Biosciences, San Diego, CA, USA) (Rodrigues *et al.,* 2017).

2.11 Anti-T. cruzi immunoglobulins assay

Specific anti-*T. cruzi* type G immunoglobulins (IgG) were detected by enzyme-linked immunosorbent assay (ELISA) as previously reported (Felizardo *et al.,* 2018). The same serum samples prepared to quantify cTnI was used in this assay. Briefly, 96-wells polystyrene microplates were sensitized with *T. cruzi* antigens and incubated with serum samples (50 µl) from each animal. Total anti-mouse immunoglobulin G (IgG), IgG1, IgG2a, and IgG2b conjugated with peroxidase (Bethyl Laboratories, Montgomery, TX, USA) were applied to the pre-sensitized wells. After treatment with the substrate (O-fenilenodiamino-OPD), the optical density was read at 490 nm in a microplate spectrophotometer (Anthos Zenyth 200; Biochrom, Cambridge, UK). Anti-IgG detection antibodies were omitted from control reactions and absorbances were subtracted from the final results.

2.12 Statistical method

The results were presented as mean and standard deviation of the mean (mean ± S.D.) or median and interquartile interval. Data distribution was verified according to the D'Agostino-Pearson's K2 normality method. Data with normal distribution were compared using one-way analysis of variance (ANOVA) followed by the Student-Newman-Keuls *post-hoc* test. Non-parametric data were compared from the Kruskal-Wallis test followed by the Student-Newman-Keuls method. Results with $P \leq 0.05$ were admitted as statistically significant.

3 RESULTS

As indicated in Fig. 1, prepatent period was similar in all infected groups. The peak of parasitemia was observed 6 days post-infection in Bz-treated mice and 8 days post-infection in INF, DNP1 and DNP2 animals. Blood parasitism was similar in INF and DNP1 mice. This parameter was efficiently controlled by Bz, but aggravated in DNP2 animals (Fig. 1A). *T. cruzi* DNA was identified in the heart of all infected animals, confirming the infection and organ parasitism (Fig. 1B). In addition, parasite load was increased in both DNP-treated groups (DNP1 and DNP2) compared to the group INF ($P<0.05$). This parameter was higher in DNP2 compared to DNP1 animals ($P<0.05$). Parasite load was attenuated in Bz-treated mice compared to the other groups ($P<0.05$) (Fig. 1B).

Figure 1 - Parasitemia curve (A) and cardiac parasite load (B)

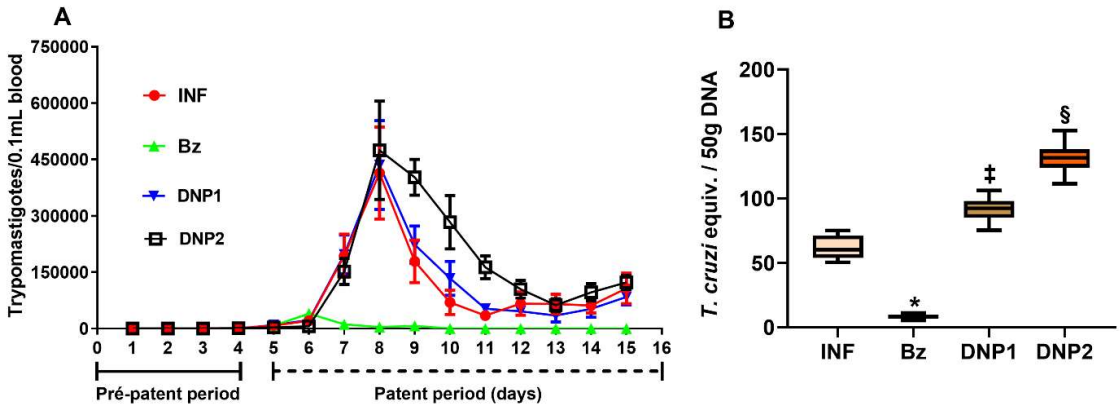

Source: From the author.

Caption: Parasitemia curve (A) and cardiac parasite load (B) in Trypanosoma cruzi-infected mice untreated and treated with 2,4-dinitrophenol (DNP) and benznidazole (Bz). Groups: UU= Uninfected untreated; INF=Infected untreated; Bz= Infected treated with 100 mg/kg Bz; DNP1= Infected treated with 5 mg/kg DNP; DNP2= Infected treated with 10 mg/kg DNP. Data are expressed as mean and standard deviation (A) or median and interquartile interval (B). Statistical difference among the groups ($P<0.05$), compared to * INF, DNP1 and DNP2; † DNP1, ‡ INF and DNP2; § INF.

As indicated in Table 1, initial parasitemia and parasitemia peak were similarly high in the groups INF, DNP1 and DNP2 ($P>0.05$), but markedly reduced in Bz-treated mice ($P<0.05$). Mean and final parasitemia were reduced in Bz-treated mice ($P<0.05$) and increased in DNP2 mice ($P<0.05$) compared to the other groups.

Table 1 - Parasitemia in *Trypanosoma cruzi*-infected mice untreated and treated with 2,4-dinitrophenol (DNP) and benznidazole (Bz).

Group	IP (Par. / 0.1 mL blood)	MP (Par. / 0.1 mL blood)	PP (Par. / 0.1 mL blood)	FP (Par. / 0.1 mL blood)
INF	74314 ± 67256	110979 ± 110194	413611 ± 367718	75111 ± 88010
Bz	19600 ± 11784*	6363 ± 4326*	3900 ± 1791*	0.00 ± 0.00*
DNP1	53828 ± 42356	117497 ± 95783	435222 ± 354044	55468 ± 51337
DNP2	76416 ± 63212	165818 ± 109749†	474550 ± 413544	93375 ± 67173†

Source: From the author.

Caption: IP= Initial parasitemia (days 5-7 post-infection); MP= Mean parasitemia (days 5-15 post-infection); PP= Peak of parasitemia (day 8 post-infection); FP= Final parasitemia (days 12-15 post-infection). Groups: INF= Infected untreated; Bz= Infected treated with 100 mg/kg Bz; DNP1= Infected treated with 5 mg/kg DNP; DNP2= Infected treated with 10 mg/kg DNP. Data are expressed as mean ± standard deviation. Statistical difference among the groups ($P<0.05$), compared to * INF, DNP1 and DNP2; † DNP1.

As shown in Fig. 2, ROS and NO production was upregulated in all infected groups compared to uninfected control animals ($P<0.05$). ROS and NO heart levels were down-regulated in the groups DNP1 and especially DNP2 compared to the groups Bz and INF ($P<0.05$). ROS and NO levels were markedly reduced in Bz-treated mice compared to the other infected groups ($P<0.05$).

Figure 2 - Reactive oxygen species (ROS) and nitrite/nitrate (NO_2^-/NO_3^-)

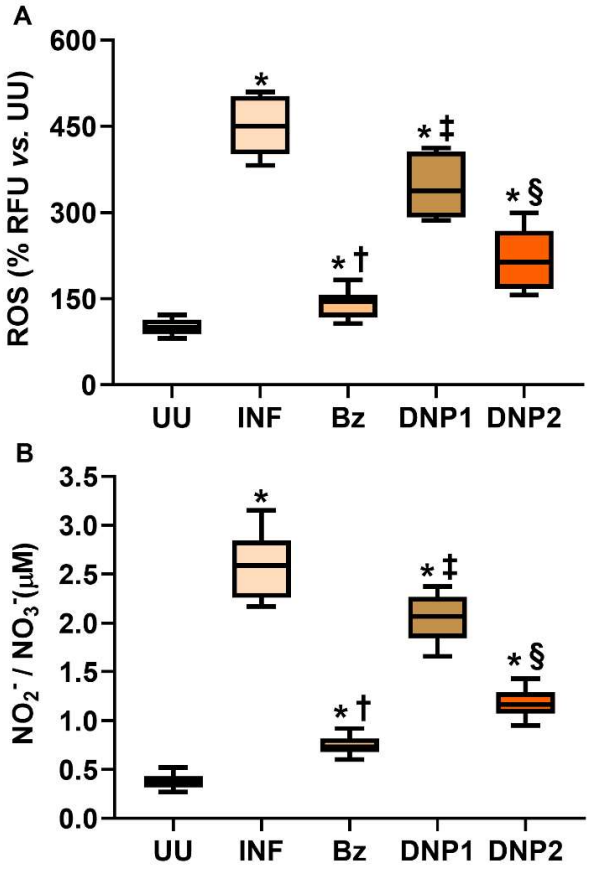

Source: From the author.

Caption: Reactive oxygen species (ROS) and nitrite/nitrate (NO_2^-/NO_3^-) heart levels in uninfected and *Trypanosoma cruzi*-infected mice untreated and treated with 2,4-dinitrophenol (DNP) and benznidazole (Bz). Groups: UU= Uninfected untreated; INF= Infected untreated; Bz= Infected treated with 100 mg/kg Bz; DNP1= Infected treated with 5 mg/kg DNP; DNP2= Infected treated with 10 mg/kg DNP. Data are expressed as median and interquartile interval. Statistical difference among the groups ($P < 0.05$), compared to * UU; † INF, DNP1 and DNP2; ‡ INF; # Bz; § INF and DNP1.

As shown in Fig. 3, MDA and PCN heart levels were upregulated in all infected groups compared to uninfected control animals ($P<0.05$). MDA and PCN levels were similarly increased in the groups INF and DNP1 ($P>0.05$). MDA and PCN levels were down-regulated in the groups DNP2 and especially Bz compared to the groups INF and DNP1 ($P<0.05$).

Figure 3 - Malondialdehyde - MDA (A) and protein carbonyl - PCN (B)

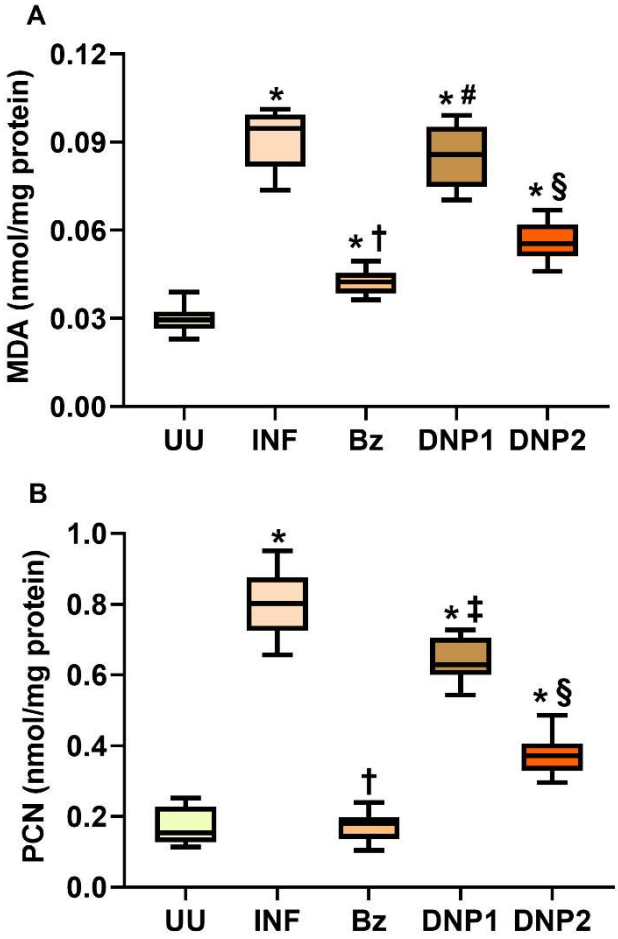

Source: From the author.

Caption: Malondialdehyde - MDA (A) and protein carbonyl - PCN (B) heart levels in uninfected and *Trypanosoma cruzi*-infected mice untreated and treated with 2,4-dinitrophenol (DNP) and benznidazole (Bz). Groups: UU= Uninfected untreated; INF= Infected untreated; Bz= Infected treated with 100 mg/kg Bz; DNP1= Infected treated with 5 mg/kg DNP; DNP2= Infected treated with 10 mg/kg DNP. Data are expressed as median and interquartile interval. Statistical difference among the groups ($P < 0.05$), compared to * UU; † INF, DNP1 and DNP2; ‡ INF; # Bz; § INF and DNP1.

As represented in Fig. 4, the microstructural analysis indicated that the heart of uninfected and *T. cruzi*-infected mice receiving Bz presented a normal myocardial structure with scarce connective tissue and interstitial cellularity, parallel and well-defined cardiomyocytes with no evidence of cell degeneration or myocarditis. Conversely, DNP1 and DNP2 animals exhibited marked myocarditis, characterized evident inflammatory infiltrate rich in mononuclear cells and notorious connective tissue expansion. These pathological changes were more pronounced in the groups DNP1 and especially DNP2. Large inflammatory foci and multiple intracellular *T. cruzi* nests were more frequently observed in DNP2 animals. The histopathological score corroborated the microstructural findings,

indicating that the pathological remodeling was more pronounced in DNP1 and DNP2 mice (Fig. 4, field diagram – FD).

Figure 4 - Representative microscopic images and histopathological score

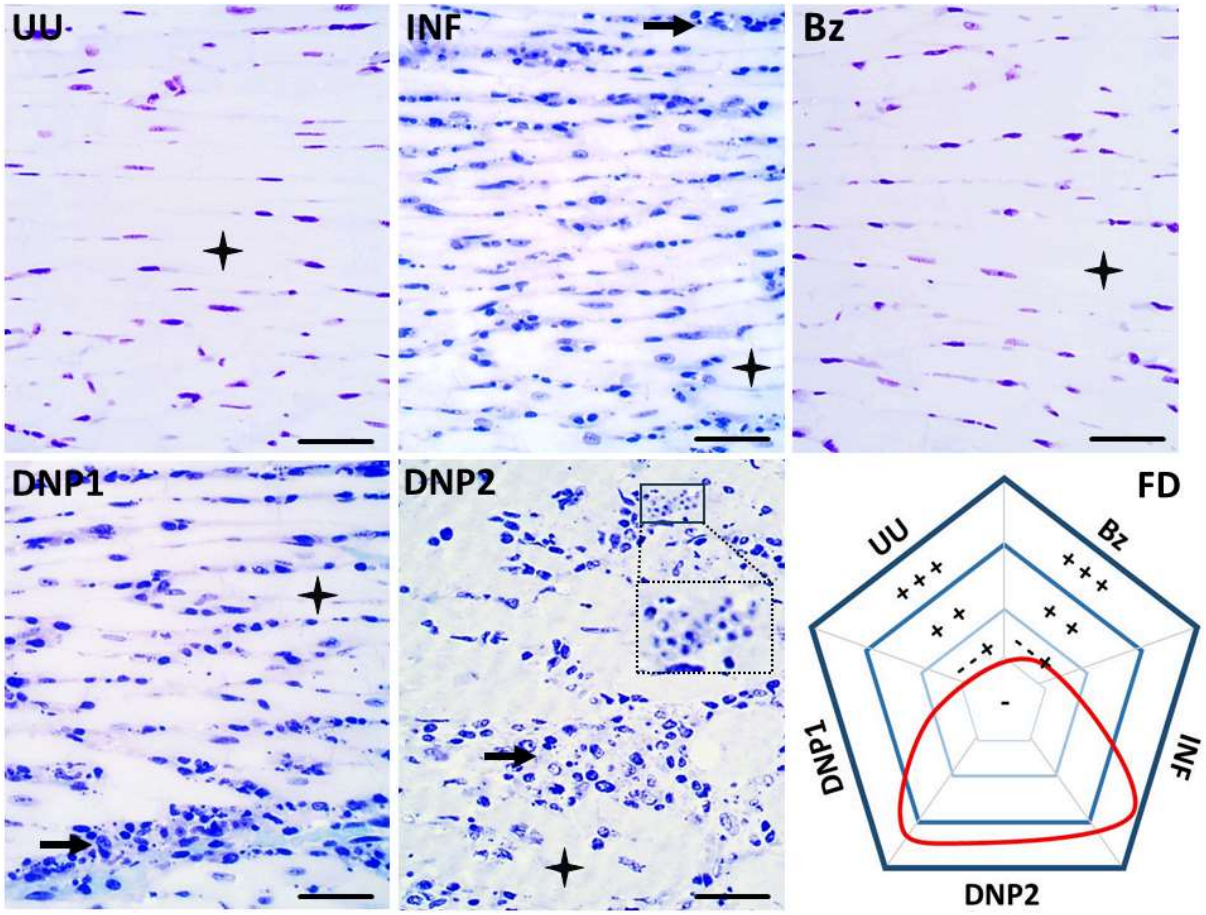

Source: From the author.

Caption: Representative microscopic images and histopathological score (Field diagram – FD) of heart from uninfected and *Trypanosoma cruzi*-infected mice untreated and treated with 2,4-dinitrophenol (DNP) and benznidazole (Bz). Groups: UU= Uninfected untreated; INF= Infected untreated; Bz= Infected treated with 100 mg/kg Bz; DNP1= Infected treated with 5 mg/kg DNP; DNP2= Infected treated with 10 mg/kg DNP. In the Field diagram (FD), the symbols indicate (-) normal, (- - +) mild, (+ +) moderate or (+ + +) intense heart damage represented by cellularity/inflammatory infiltrate, myocardial disorganization, cardiomyocytes hypertrophy and necrosis. The area delimited by the red line indicates the histopathological score determined by all groups, and the line direction indicates the influence of each group in this status. No evidence of heart inflammation was observed in uninfected untreated mice and infected animals receiving Bz (predominance of normal [-] or mild [- - +] cellularity).

As shown in Fig. 5, NAG and MPO activities were upregulated in the heart of INF, DNP1 and DNP2 animals compared to uninfected and Bz-treated mice ($P<0.05$). MPO activity was similarly increased in the groups INF and DNP1 ($P>0.05$). MPO activity was

similarly reduced in uninfected and Bz-treated mice compared to the other groups (P>0.05). NAG and MPO activities were down-regulated in the heart of DNP2 compared to DNP1 mice (P<0.05).

Figure 5 - N-acetyl-β-D-glucosaminidase - NAG (A) and myeloperoxidase - MPO (B)

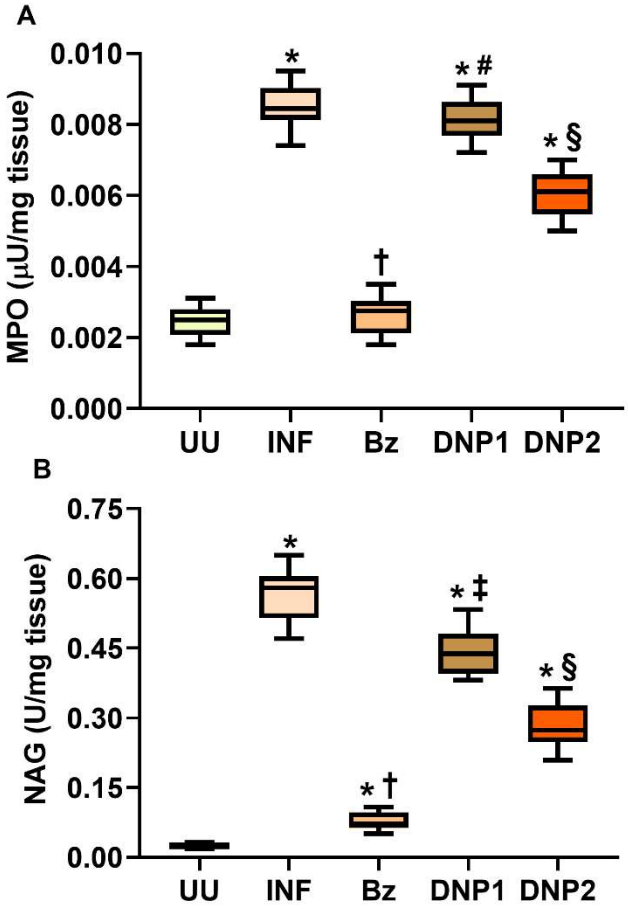

Source: From the author.

Caption: N-acetyl-β-D-glucosaminidase - NAG (A) and myeloperoxidase - MPO (B) activity in the heart of uninfected and *Trypanosoma cruzi*-infected mice untreated and treated with 2,4-dinitrophenol (DNP) and benznidazole (Bz). Groups: UU= Uninfected untreated; INF= Infected untreated; Bz= Infected treated with 100 mg/kg Bz; DNP1= Infected treated with 5 mg/kg DNP; DNP2= Infected treated with 10 mg/kg DNP. Data are expressed as median and interquartile interval. Statistical difference among the groups (P <0.05), compared to * UU; † INF, DNP1 and DNP2; ‡ INF; # Bz; § INF and DNP1.

Myocardial cellularity and cTnI circulating levels are shown in Fig. 6. These parameters were upregulated in INF, DNP1 and DNP2 animals compared to uninfected and Bz-treated mice (P<0.05). Myocardial cellularity was similar in uninfected and Bz-treated animals (P>0.05), and reduced in DNP2 mice compared to the groups INF and DNP1 (P<0.05). cTnI levels were increased in all infected groups compared to uninfected control

animals (P<0.05). This marker was upregulated in DNP1 and DNP2 animals compared to the other groups (P<0.05). DNP2 mice exhibited higher cTnI levels compared to DNP1 animals (P<0.05).

Figure 6 - Interstitial myocardial cellularity (IC - A) and cardiac troponin I (cTnI) circulating levels (B)

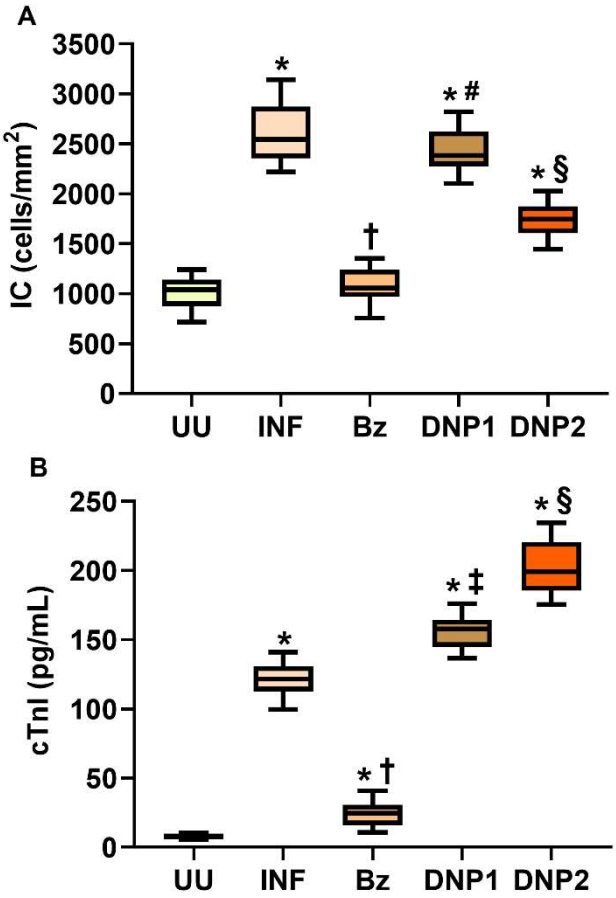

Source: From the author.

Caption: Interstitial myocardial cellularity (IC - A) and cardiac troponin I (cTnI) circulating levels (B) in uninfected and *Trypanosoma cruzi*-infected mice untreated and treated with 2,4-dinitrophenol (DNP) and benznidazole (Bz). Groups: UU= Uninfected untreated; INF= Infected untreated; Bz= Infected treated with 100 mg/kg Bz; DNP1= Infected treated with 5 mg/kg DNP; DNP2= Infected treated with 10 mg/kg DNP. Data are expressed as median and interquartile interval. Statistical difference among the groups (P <0.05), compared to * UU; † INF, DNP1 and DNP2; ‡ INF; # Bz; § INF and DNP1.

As shown in Fig. 7, IFN-γ, TNF, MCP-1/CCL2 and IL-10 heart levels were upregulated in INF, DNP1 and DNP2 animals compared to uninfected and Bz-treated mice (P<0.05). Only MCP-1/CCL2 levels were similar in uninfected mice and those infected receiving Bz (P>0.05). IFN-γ, TNF, MCP-1/CCL2 and IL-10 levels were similar in DNP1 and DNP2 mice

(P>0.05). These immunological effectors were reduced in DNP2 animals compared to the groups INF and DNP1 (P<0.05).

Figure 7 - Cytokine heart levels in *Trypanosoma cruzi*-infected mice untreated and treated with 2,4-dinitrophenol (DNP) and benznidazole (Bz).

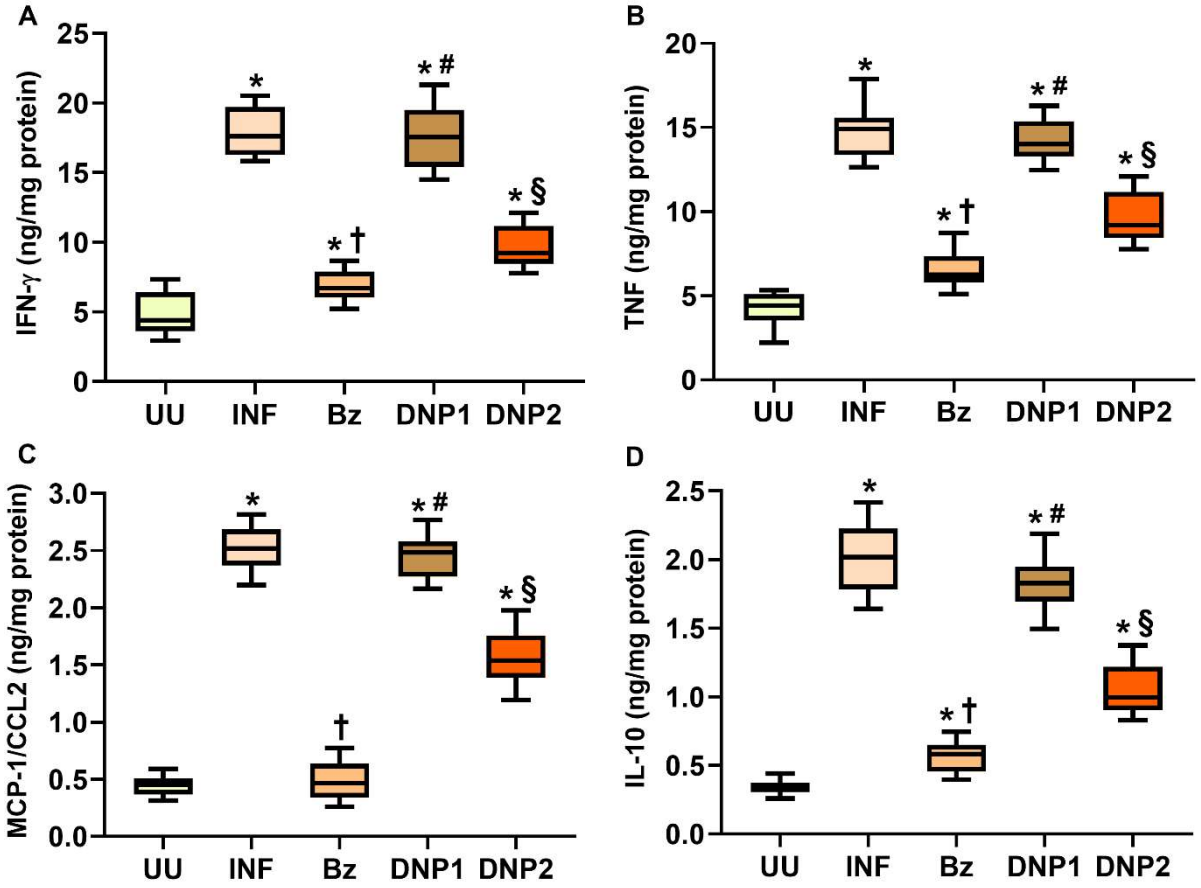

Source: From the author.

Caption: Cytokine heart levels in *Trypanosoma cruzi*-infected mice untreated and treated with 2,4-dinitrophenol (DNP) and benznidazole (Bz). Groups: UU= Uninfected untreated; INF= Infected untreated; Bz= Infected treated with 100 mg/kg Bz; DNP1= Infected treated with 5 mg/kg DNP; DNP2= Infected treated with 10 mg/kg DNP. Data are expressed as median and interquartile interval. Statistical difference among the groups (P<0.05), compared to * UU; † INF, DNP1 and DNP2; ‡ INF; # Bz; § INF and DNP1.

Anti-*T. cruzi* IgG titers are indicated in Fig. 7. Total IgG, IgG1, IgG2a and IgG2b titers were upregulated in all infected groups compared to control uninfected animals (P<0.05). Total IgG and IgG1 were down-regulated in the groups DNP1, DNP2 and Bz compared to the group INF (P<0.05). Except for IgG2b, all IgG subclasses were reduced in DNP2 compared to DNP1 mice (P<0.05), and even more reduced in Bz-treated mice compared to these groups

(P<0.05). IgG2a and IgG2b titers were similar in the groups INF and DNP1 (P>0.05). IgG2a titers were reduced in DNP2 compared to the groups INF and DNP1 (P<0.05).

Figure 8 - Immunoglobulin G (IgG) circulating levels in *Trypanosoma cruzi*-infected mice untreated and treated with 2,4-dinitrophenol (DNP) and benznidazole (Bz).

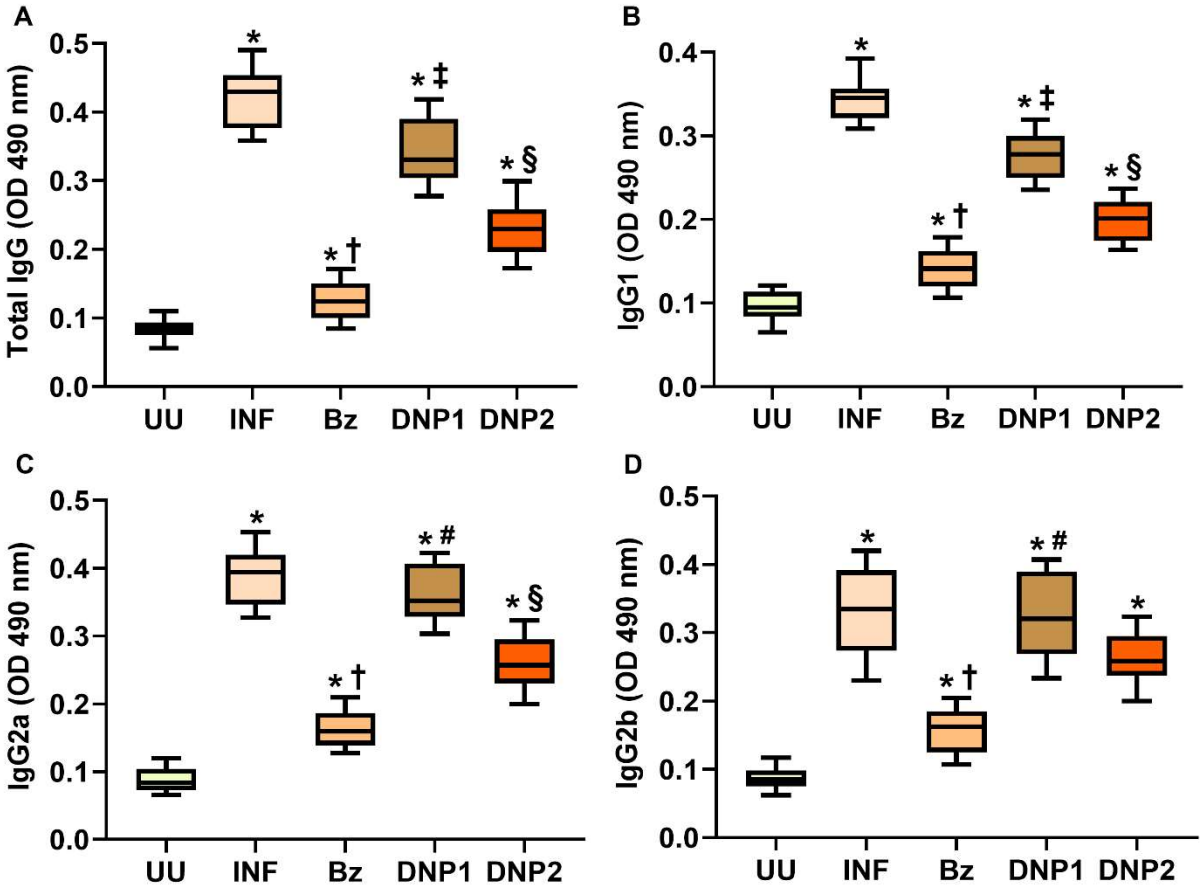

Source: From the author.

Caption: Immunoglobulin G (IgG) circulating levels in *Trypanosoma cruzi*-infected mice untreated and treated with 2,4-dinitrophenol (DNP) and benznidazole (Bz). Groups: UU= Uninfected untreated; INF= Infected untreated; Bz= Infected treated with 100 mg/kg Bz; DNP1= Infected treated with 5 mg/kg DNP; DNP2= Infected treated with 10 mg/kg DNP. Data are expressed as median and interquartile interval. Statistical difference among the groups (P <0.05), compared to * UU; † INF, DNP1 and DNP2; ‡ INF; # Bz; § INF and DNP1.

4 DISCUSSION

In the present study, we identified for the first time that DNP modulates *T. cruzi* infection, cardiac parasitism and myocarditis in mice, exerting effects opposite to reference antiparasitic chemotherapy. Accordingly, DNP administration aggravated parasitemia and/or heart parasitism, which were effectively controlled by Bz. Interestingly, blood and heart parasitism exhibited similar behavior only at the highest DNP dose, which was not observed in animals receiving the lowest dose of this drug. In *T. cruzi* infection, parasitemia and cardiac parasite load are not invariably correlated. Although this dependence is expected considering *T. cruzi* replicative cycle and myotropic lineages (e.g., CL and Colombiana), parasite tropism is widely variable in different *T. cruzi* strains (Melo; Brener, 1978; Andrade; Magalhães, 1997). Thus, the dissociation between parasitemia and cardiac parasitism in macrophagotropic parasites is not uncommon, as occurs with the Y strain (Melo; Brener, 1978; Andrade; Magalhães, 1997). In addition, marked parasitism and organ damage can occur even in the absence of high parasitemia (Higuchi *et al.,* 1993; Caldas *et al.,* 2019). On the other hand, our findings indicate that parasitemia and cardiac parasitism may be aligned even in infections caused by a macrophagotropic strain, which may be linked to the worsening of *T. cruzi* infection according to Felizardo *et al.* (2018), Novaes *et al.* (2018) e Mendonça *et al.* (2020) in response to the high DNP dose used (10 mg/kg). Unlike DNP, parasitemia and heart parasitism were simultaneously attenuated in Bz-treated mice, reinforcing the use of Bz as reference drug, since parasitological control is the primary outcome expected in the effective management of acute Chagas disease (Santos *et al.,* 2015; Novaes *et al.,* 2016; Caldas *et al.,* 2019).

As expected, ROS and NO production were upregulated in the heart of *T. cruzi*-infected mice. There is consistent evidence indicating that the heart is a direct source and simultaneous target of the redox imbalance triggered by *T. cruzi* infection (Wen; Garg, 2008; Gupta *et al.,* 2009; Rodrigues *et al.,* 2017). Accordingly, reactive species derive from two main cardiac sources, represented by the disruption of the electron transport chain in infected cardiomyocytes as described by Wen; Garg, (2008), Gupta *et al.* (2009) and by the respiratory burst in leukocytes recruited and activated in the heart to combat cell parasitism (Paiva; Bozza, 2014; Nogueira *et al.,* 2023). Despite the antiparasitic effects, the nonspecific cytotoxicity of these reactive effectors contributes to aggravating cardiac injury according to Paiva *et al.* (2018), adding to the damage caused by direct lysis of *T. cruzi* parasitized cells in acute infections (Zacks *et al.,* 2005; Paiva *et al.,* 2018). MDA and PCN cardiac levels

confirmed redox imbalance and oxidative stress in infected animals, indicating that heart lipids and proteins are sensitive targets of reactive effectors in Chagas disease (Novaes *et al.,* 2015; Santos *et al.,* 2015; Mendonça *et al.,* 2020). As expected, Bz and DNP attenuated reactive species biosynthesis and molecular oxidation in infected animals. However, the impact of this drug on parasitemia and cardiac parasitism indicates that the observed antioxidant responses are linked to distinct pharmacological properties of these drugs. Accordingly, there is evidence that oxidative stress attenuation is a secondary response to treatment of *T. cruzi*-infected animals with Bz (Santos *et al.,* 2015; Novaes *et al.,* 2018; Mendonça *et al.,* 2020). In this sense, parasitological control is accompanied by a reduction in antigenic load and immunostimulation, resulting in attenuation of myocarditis (e.g., leukocytes recruitment and cytokines production) and the associated redox imbalance (Santos *et al.,* 2015; Novaes *et al.,* 2018; Mendonça *et al.,* 2020). On the contrary, the antiparasitic ineffectiveness reinforces the classic antioxidant mechanism attributed to DNP, which attenuates reactive species biosynthesis through partial uncoupling of the mitochondrial respiratory chain in eukaryotic cells (Nasab *et al.,* 2004; Geisler, 2019). Although blocking oxidative stress is proposed as a complementary alternative to attenuate cardiac damage associated with *T. cruzi* infection as described by Novaes *et al.* (2016), Vilar-Vereira *et al.* (2016) e Tieghi *et al.* (2017), antioxidant therapy is still controversial. Thus, the use of free radicals scavengers such as vitamin C and E has not always been associated with relevant protective effects in acute Chagas disease (Gusmão *et al.,* 2012; Marin *et al.,* 2012; Novaes *et al.,* 2017).

Surprisingly, reactive species production and molecular oxidation were consistent with myocardial microstructure in both untreated and Bz-treated infected animals. Considering myocardial cellularity, these intriguing findings reinforce the proposition that BZ-induced parasitological and inflammation control was associated with the attenuation of cardiac oxidative stress. Furthermore, only the highest DNP dose was effective in down-regulating myocardial cellularity, indicating that this drug may have dose-dependent effects on leukocyte recruitment in *T. cruzi* infection. However, cardiac MPO and/or NAG activities were reduced in animals receiving all DNP doses, indicating that neutrophils and macrophages activation may be especially impaired by this drug, even when administered at lower concentrations. MPO according to Gupta *et al.* (2009), Machado *et al.* (2012) and NAG according to Silva *et al.,* (2015); Mendonça *et al.* (2020) are respective markers of the innate defense responses mediated by neutrophils and macrophages against pathogens, so that cardiac up-regulation of these enzymes is expected in Chagas disease (Mendonça *et al.,* 2020;

Pereira-Santos *et al.,* 2022). ROS and RNS produced by neutrophils and macrophages play a central antiparasitic role in *T. cruzi*-infected organs, which is impaired by inhibitory drugs (Mendonça *et al.,* 2020). As only the highest DNP dose simultaneously down-regulated myocardial cellularity, MPO and NAG activity, it is not unrealistic to assume that the mechanisms that regulate neutrophils and macrophages activation may be more susceptible to DNP than those involved in cardiac leukocyte recruitment. Although this proposition needs to be clarified, there is evidence that mitochondrial uncouplers such as DNP inhibit macrophages activation second study by Cifarelli *et al.* (1979), Patoli *et al.* (2020) by stimulating mitophagy in these cells (Patoli *et al.,* 2020). Thus, this process may be also related to ROS down-regulation, a phenomenon that impairs classical macrophages (M1) activation according to Patoli *et al.* (2020), which are essential in controlling the parasite load in *T. cruzi* infection (Zanluqui *et al.,* 2015; Rodrigues *et al.,* 2017). Despite the reduced inflammatory infiltrate, MPO and NAG activities, DNP treatment was associated with increased cTnI circulating levels. These findings indicate greater cardiomyocytes damage, which may be related to the worsening of direct injuries caused by cardiomyocytes parasitism according to Gonçalves-Santos *et al.* (2023), representing an outcome consistent with the greater parasite load in DNP-exposed animals. Conversely, cTnI levels were markedly attenuated in Bz-treated mice. This finding was consistent with parasitemia, parasite load and oxidative stress down-regulation in these animals, reinforcing that cardiomyocytes integrity is dependent of an adequate parasitological and oxidative control in Chagas disease (Gonçalves-Santos *et al.,* 2023; Nogueira *et al.,* 2023).

Interestingly, reduced leukocytes activity can be corroborated by cytokines down-regulation in animals treated with the highest DNP dose. Accordingly, attenuation in IFN-γ and TNF biosynthesis has special relevance for the worsening of parasitemia and cardiac parasitism in DNP-treated animals. High IFN-γ and TNF levels are typically produced in Th1-polarized immunological response, which is essential to improve host resistance against *T. cruzi* (Machado *et al.,* 2012, 2013; Rodrigues *et al.,* 2017). As these Th1 cytokines reinforce parasitological control in target organs, it was already expected that attenuated IFN-γ and TNF production would worsen parasitism and cardiac microstructural damage as described by Machado *et al.* (2012, 2013), Felizardo *et al.* (2018), corroborating our findings. There is evidence that IFN-γ and TNF have antiparasitic effects by stimulating leucocytes recruitment and activation in infected organs, inducing classical macrophages polarization and oxidative burst in mononuclear and polymorphonuclear immune cells (Gupta *et al.,* 2009; Machado *et al.,* 2013). In these processes, IFN-γ and TNF trigger ROS (e.g.,

H_2O_2, HClO, $O2^{\bullet-}$, and $OH^{\bullet-}$) and RNS production (e.g., NO and $ONOO^{\bullet-}$) (mariappan *et al.,* 2007; prasanna *et al.,* (2007), which neutralize *T. cruzi* by oxi-reduction processes (Gupta *et al.,* 2009; Machado *et al.,* 2013). Accordingly, in addition to direct mitochondrial uncoupling, reactive species down-regulation may be linked to the attenuated Th1 phenotype in DNP-treated animals. Thus, hosts become more susceptible to cardiac parasitism, since these oxidative and immunological effectors are natural barriers against *T. cruzi* (Gupta *et al.,* 2009; Machado *et al.,* 2012, 2013). As expected, IFN and TNF levels were further reduced by Bz treatment. However, these effects are mediated by two different and complementary mechanisms, represented by anti-inflammatory (linked to NF-κB inhibition) and direct antiparasitic responses triggered by Bz (RONCO et al., 2011). Taken together, these pharmacological properties are highly relevant and desirable in anti-*T. cruzi* drugs, determining efficient control of the parasite load and *T. cruzi*-induced acute myocarditis (Cevey *et al.,* 2015; Mendonça *et al.,* 2020; Vilas-Boas *et al.,* 2022).

As well as IFN-γ and TNF, MCP-1/CCL2 and IL-10 heart levels were increased by *T. cruzi* infection, which were attenuated in animals receiving Bz and the highest DNP dose. It is recognized that the chemokine MCP-1/CCL2 plays an important protective role against *T. cruzi*, specially by stimulating macrophages recruitment and upregulating the inducible nitric oxide synthase/nitric oxide system in parasitized organs (Ramasawmy *et al.,* 2006; Paiva *et al.,* 2009). In addition, high production of this chemokine is often associated with intense myocarditis and oxidative damage in acute Chagas disease according to Ramasawmy *et al.* (2006), Paiva *et al.* (2009), as observed in infected untreated mice. Thus, MCP-1/CCL2 down-regulation by Bz and DNP is consistent with attenuation of the inflammatory infiltrate and cardiomyocytes injury, as respectively indicated by the reduction in myocardial cellularity and cTnI levels. Unlike IFN-γ, TNF and MCP-1/CCL2, IL-10 is an Treg anti-inflammatory effector without antiparasitic activity (Abrahamsohn *et al.,* 1996; Rada *et al.,* 2020). In Chagas disease, IL-10 is upregulated as a counterregulatory response that modulates the intensity of the Th1 phenotype, preventing exacerbated inflammation and oxidative tissue damage in parasitized organs (Abrahamsohn *et al.,* 1996; Rada *et al.,* 2020). Accordingly, IL-10 deficiency is associated with immune hyperactivity and more severe myocarditis in mice, determining higher mortality rates in *T. cruzi*-infected animals (Hunter *et al.,* 1997; Roffê *et al.,* 2012). Typically, MCP-1 and IL-10 down-regulation is associated with effective parasitological control induced by Bz (Santos *et al.,* 2019; Mendonça *et al.,* 2020). However, it may represent a direct inhibitory response to DNP treatment, which needs to be further clarified.

As expected, the immunological reaction to *T. cruzi* infection was consistent with a concomitant upregulation of anti-*T. cruzi* immunoglobulins. There is evidence that cell mediated immunological responses are the main line of defense against intracellular pathogens, including *T. cruzi* (Abrahamsohn *et al.,* 1996; Machado *et al.,* 2013). However, humoral mechanisms reinforce host resistance to *T. cruzi* by signaling infected cells to be destroyed and neutralizing parasites (e.g., activating the complement system) released into the extracellular space (Pyrrho *et al.,* 1998; Bryan *et al.,* 2010). Classically, protective humoral responses against *T. cruzi* have been mainly attributed to the production of neutralizing antibodies of the IgG2a subclass (Pyrrho *et al.,* 1998; Bryan *et al.,* 2010). However, similar lytic effects triggered by IgG1 indicate that both immunoglobulins play relevant role in controlling *T. cruz*i infection (Pyrrho *et al.,* 1998; Bryan *et al.,* 2010). Curiously, intense production of humoral effectors is not invariably associated with protective responses in *T. cruz*i-infected hosts. Accordingly, non-neutralizing antibodies can interact with irrelevant antigens and block the activity of lytic antibodies, determining an ineffective humoral response (Powell; Wassom, 1993). As indicated in previous studies of Novaes *et al.* (2016), Mendonça *et al.* (2020), the downregulation in anti-*T. cruzi* IgG titers observed in the present study was consistent with reduced parasite load in Bz-treated animals. Thus, IgG production is expected to be down-regulated as the antigenic load is attenuated by the reference treatment (Gonçalves-Santos *et al.,* 2019; Mendonça *et al.,* 2020). However, DNP treatment determined a divergent humoral response, reducing IgG titers at the same time that stimulated parasite load. Although the mechanism associated with DNP-induced humoral inhibition remains unclear, this response may increase host susceptibility to heart parasitism and cardiomyocytes damage according to Kumar; Tarleton, (1998), Bryan *et al.* (2010), which may partially explain the high parasite load and cTnI levels in infected animals receiving DNP. Classically, the attenuation of the immune response is admitted as a marker of antiparasitic chemotherapy effectiveness (Machado-De-Assis *et al.,* 2012; Caldas *et al.,* 2019). However, this response is only desirable in parallel with efficient parasitological control, in the absence of which the infection can be worsened, as occurred in DNP-treated animals.

5 CONCLUSION

Taken together, our findings indicate that due to the infectivity in controlling parasitemia and parasite load, DNP may act as a risk factor for acute Chagas heart disease. Guided by Bz-based reference chemotherapy, the undesirable response to DNP treatment was especially related to the down-regulation in oxidative and immunological effectors directly involved in host resistance against *T. cruzi* infection. Accordingly, unbalanced host defenses increase heart susceptibility to parasitism and *T. cruzi*-induced cardiomyocytes microstructural damage in DNP-exposed mice. These responses contrast with Bz-induced cardioprotective effects, which were manifested by the desirable combination of direct antiparasitic and anti-inflammatory properties of this drug, culminating in a marked attenuation of myocarditis associated with heart parasitism and oxidative stress triggered by *T. cruzi* infection.

ACKNOWLEDGEMENTS

This work was supported by the following Brazilian agencies: Fundação do Amparo à Pesquisa do Estado de Minas Gerais (FAPEMIG, processes APQ-00126-18, APQ-03519-22 and APQ-04164-22) and Conselho Nacional de Desenvolvimento Científico e Tecnológico (CNPq, processes 310331/2020-0, and 311105/2020-3, 310413/2023-0, 306733/2023-4, and 403194/2023-7). This study was financed in part by the Coordenação de Aperfeiçoamento de Pessoal de Nível Superior - Brasil (CAPES, Finance code 001 e Pós-Doutorado Estratégico – Edital 16/2022, processo 88887.837841/2023-00).

REFERENCES

ABRAHAMSOHN, I. A.; COFFMAN, R. L. *Trypanosoma cruzi*: IL-10, TNF, IFN-gamma, and IL-12 regulate innate and acquired immunity to infection. **Exp Parasitol.,** v. 84, n. 2, p. 231-244, 1996.

ANDRADE, S. G.; MAGALHÃES, J. B. Biodemes and zymodemes of *Trypanosoma cruzi* strains: correlations with clinical data and experimental pathology. **Rev Soc Bras Med Trop.,** v. 30, n. 1, p. 27-35, 1997.

BHATTACHARJEE, S. *et al.* Phytochemical and pharmacological evaluation of methanolic extract of *Lathyrus sativus* L. seeds. **Clin Phytosci.,** v. 4, n. 20, 2018.

BRENER, Z. Therapeutic activity and criterion of cure on mice experimentally infected with *Trypanosoma cruzi*. **Rev Inst Med Trop Sao Paulo.,** v. 4, p. 389-396, 1962.

BRYAN, M. A.; GUYACH, S. E.; NORRIS, K. A. Specific humoral immunity versus polyclonal B cell activation in *Trypanosoma cruzi* infection of susceptible and resistant mice. **PLoS Negl Trop Dis.,** v. 4, n. 7, p. 733, 2010.

BROWN, R. K.; KELLY, F. J. Peroxides and other products. *In:* PUNCHARD, N. A.; KELLY, F. J. (Ed.). **Free radicals:** a practical approach. New York: Oxsford University, 1996. p.119-131.

CALDAS, I. S. *et al.* Parasitaemia and parasitic load are limited targets of the aetiological treatment to control the progression of cardiac fibrosis and chronic cardiomyopathy in *Trypanosoma cruzi*-infected dogs. **Acta Trop.,** v. 189, p. 30-38, 2019.

CALDAS, I. S.; SANTOS, E. G.; NOVAES, R. D. An evaluation of benznidazole as a Chagas disease therapeutic. **Expert Opin Pharmacother.,** v. 20, n. 15, p. 1797-1807, 2019.

CEVEY, A. C. *et al.* Low-dose benznidazole treatment results in parasite clearance and attenuates heart inflammatory reaction in an experimental model of infection with a highly virulent Trypanosoma cruzi strain. **Int J Parasitol Drugs Drug Resist.,** v. 6, n. 1, p. 12-22, 2015.

CIFARELLI, A. *et al.* The influence of some metabolic inhibitors on phagocytic activity of mouse macrophages in vitro. **Res Exp Med.,** v. 174, n. 2, p. 197-204, 1979.

DIAS, P. P. *et al.* Cardiomyocyte oxidants production may signal to *T. cruzi* intracellular development. **PLoS Negl Trop Dis**. v. 11, n. 8, 2017.

DINIZ, L. F. *et al.* Outcome of E1224-Benznidazole Combination Treatment for infection with a multidrug-resistant *Trypanosoma cruzi* strain in mice. **Antimicrob Agents Chemother.,** v. 62, n. 6, 2018.

ECHEVERRÍA, L. E. *et al*. WHF IASC Roadmap on Chagas disease. **Glob Heart.,** v. 15, n. 1, p. 26, 2020.

FELIZARDO, A. A. *et al.* Impact of *Trypanosoma cruzi* infection on nitric oxide synthase and arginase expression and activity in young and elderly mice. **Free Radic Biol Med.,** v. 129, p. 227-236, 2018.

GEISLER, J. G. 2,4 Dinitrophenol as medicine. **Cells.,** v. 8, n. 3, p. 280, 2019.

GOES, G. R. *et al. Trypanosoma cruzi* needs a signal provided by reactive oxygen species to infect macrophages. **PLoS Negl Trop Dis.,** v. 10, n. 4, 2016.

GONÇALVES-SANTOS, E. *et al.* Sesquiterpene lactone potentiates the immunomodulatory, antiparasitic and cardioprotective effects on anti-*Trypanosoma cruzi* specific chemotherapy. **Int Immunopharmacol.,** v. 77, 2019.

GUHL, F.; RAMÍREZ, J. D. Poverty, migration, and Chagas disease. **Curr Trop Med Rep.,** v. 8, p. 52-58, 2021.

GUPTA, S.; WEN, Jian-Jun.; GARG, N. J. Oxidative stress in Chagas disease. **Interdiscip Perspect Infect Dis.,** v. 2009, 2009.

GUSMÃO, A. S. *et al.* Vitamin C effects in mice experimentally infected with *Trypanosoma cruzi* QM2 strain. **Rev Soc Bras Med Trop.,** v. 45, n. 1, p. 51-54, 2012.

HIGUCHI, M. L. *et al.* Correlation between *Trypanosoma cruzi* parasitism and myocardial inflammatory infiltrate in human chronic chagasic myocarditis: Light microscopy and immunohistochemical findings. **Cardiovasc Pathol.,** v. 2, n. 2, p. 101-106, 1993.

HUNTER, C. A. IL-10 is required to prevent immune hyperactivity during infection with Trypanosoma cruzi. **J Immunol.,** v. 158, n. 7, p. 3311-3316, 1997.

IGOILLO-ESTEVE, M. *et al.* The pentose phosphate pathway in *Trypanosoma cruzi*: A potential target for the chemotherapy of Chagas disease. **An Acad Bras Cienc.,** v. 79, n. 4, p. 649-663, 2007.

IVANOVA, N. *et al.* New insights into blue light phototherapy in experimental *Trypanosoma cruzi* infection. **Front Cell Infect Microbiol.,** v. 11, 2021.

KUMAR, S.; TARLETON, R. L. The relative contribution of antibody production and CD8+ T cell function to immune control of *Trypanosoma cruzi*. **Parasite Immunol.,** v. 20, n. 5, p. 207-216, 1998.

MACHADO-DE-ASSIS. G. F. *et al.* Posttherapeutic cure criteria in Chagas' disease: conventional serology followed by supplementary serological, parasitological, and molecular tests. **Clin Vaccine Immunol.,** v. 19, n. 8, p. 1283-1291, 2012.

MACHADO, F. S. *et al.* Current understanding of immunity to *Trypanosoma cruzi* infection and pathogenesis of Chagas disease. **Semin Immunopathol.,** v. 34, n. 6, p. 753-770, 2012.

MACHADO. F. S.; TANOWITZ, H. B.; RIBEIRO, A. L. Pathogenesis of chagas cardiomyopathy: role of inflammation and oxidative stress. **J Am Heart Assoc.,** v. 2, n. 5, 2013.

MALDONADO, E. *et al.* The use of antioxidants as potential co-adjuvants to treat chronic Chagas disease. **Antioxidants.,** v. 10, n. 7, p. 1022, 2021.

MARIAPPAN, N. *et al.* TNF-alpha-induced mitochondrial oxidative stress and cardiac dysfunction: restoration by superoxide dismutase mimetic Tempol. **Am J Physiol Heart Circ Physiol.,** v. 293, n. 5, p. 2726-2737, 2007.

MARIM, R. G. *et al.* Effects of vitamin C supplementation on acute phase Chagas disease in experimentally infected mice with *Trypanosoma cruzi* QM1 strain. **Rev Inst Med Trop Sao Paulo.,** v. 54, n. 6, p. 319-323, 2012.

MAZZETI, A. L. *et al.* Time and dose-dependence evaluation of nitroheterocyclic drugs for improving efficacy following *Trypanosoma cruzi* infection: A pre-clinical study. **Biochem Pharmacol.,** v. 148, p. 213-221, 2018.

MELO, R. C.; BRENER, Z. Tissue tropism of different Trypanosoma cruzi strains. **J Parasitol.,** v. 64, n. 3, p. 475-782, 1978.

MENDONÇA, A. A. S. *et al.* Could phenothiazine-benznidazole combined chemotherapy be effective in controlling heart parasitism and acute infectious myocarditis? **Pharmacol Res.,** v. 158, 2020.

MENDONÇA, A. A. S. *et al.* Thioridazine aggravates skeletal myositis, systemic and liver inflammation in *Trypanosoma cruzi*-infected and benznidazole-treated mice. **Int Immunopharmacol.,** v. 85, 2020.

MESQUITA, C. S. *et al.* Simplified 2,4-dinitrophenylhydrazine spectrophotometric assay for quantification of carbonyls in oxidized proteins. **Anal Biochem.,** v. 458, p. 69-71, 2014.

NASAB, M. H. F.; MANAVI, M. A.; BAEERI, M. Dinitrophenols. Encyclopedia of toxicology. v. 3, p. 825-828, 2004.

NOGUEIRA, S. S. Oxidative stress, cardiomyocytes senescence and contractile dysfunction in *in vitro* and *in vivo* experimental models of Chagas disease. **Acta Trop.,** v. 244, 2023.

NOVAES, R. D. et al. *Trypanosoma cruzi* infection and benznidazole therapy independently stimulate oxidative status and structural pathological remodeling of the liver tissue in mice. **Parasitol Res.** v. 114, n. 8, p. 2873-2881, 2015.

NOVAES, R. D. *et al.* Curcumin enhances the anti-*Trypanosoma cruzi* activity of benznidazole-based chemotherapy in acute experimental Chagas disease. **Antimicrob Agents Chemother.,** v. 60, n. 6, p. 3355-3364, 2016.

NOVAES, R. D. *et al.* Nonsteroidal anti-inflammatory is more effective than anti-oxidant therapy in counteracting oxidative/nitrosative stress and heart disease in *T. cruzi*-infected mice. **Parasitology.,** v. 144, n. 7, p. 904-916, 2017.

NOVAES, R. D. *et al.* Purinergic antagonist suramin aggravates myocarditis and increases mortality by enhancing parasitism, inflammation, and reactive tissue damage in *Trypanosoma cruzi*-Infected Mice. **Oxid Med Cell Longev.,** v. 2018, 2018.

OMIDI, F. *et al.* COVID-19 and cardiomyopathy: A systematic review. **Front Cardiovasc Med.,** v. 8, 2021.

PAIVA, C. N. *et al.* CCL2/MCP-1 controls parasite burden, cell infiltration, and mononuclear activation during acute Trypanosoma cruzi infection. **J Leukoc Biol.,** v. 86, n. 5, p. 1239-1246, 2009.

PAIVA, C. N.; BOZZA, M. T. Are reactive oxygen species always detrimental to pathogens? **Antioxid Redox Signal.,** v. 20, n. 6, p. 1000-1037, 2014.

PAIVA, C. N.; MEDEI, E.; BOZZA, M. T. ROS and *Trypanosoma cruzi*: Fuel to infection, poison to the heart. **PLoS Pathog.,** v. 14, n. 4, 2018.

PATOLI, D. *et al.* Inhibition of mitophagy drives macrophage activation and antibacterial defense during sepsis. **J Clin Invest.,** v. 130, n. 11, p. 5858-5874, 2020.

PEREIRA-SANTOS, M. *et al.* Chronic rapamycin pretreatment modulates arginase/inducible nitric oxide synthase balance attenuating aging-dependent susceptibility to *Trypanosoma cruzi* infection and acute myocarditis. **Exp Gerontol.,** p. 111676, 2022.

POWELL, M. R.; WASSOM, D. L. Host genetics and resistance to acute Trypanosoma cruzi infection in mice. I. Antibody isotype profiles. **Parasite Immunol.,** v. 15, n. 4, p. 215-221, 1993.

PRASANNA, S. J.; SAHA, B.; NANDI, D. Involvement of oxidative and nitrosative stress in modulation of gene expression and functional responses by IFNgamma. **Int Immunol.,** v. 19, n. 7, p. 867-879, 2007.

PYRRHO, A. S,. *et al.* Trypanosoma cruzi: IgG1 and IgG2b are the main immunoglobulins produced by vaccinated mice. **Parasitol Res.,** v. 84, n. 4, p. 333-337, 1998.

RADA, J. *et al.* IL-10-Dependent and -Independent Mechanisms Are Involved in the Cardiac Pathology Modulation Mediated by Fenofibrate in an Experimental Model of Chagas Heart Disease. **Front Immunol.,** v. 11, 2020.

RAMASAWMY, R. *et al.* The monocyte chemoattractant protein-1 gene polymorphism is associated with cardiomyopathy in human chagas disease. **Clin Infect Dis.,** v. 43, n. 3, p. 305-311, 2006.

RODRIGUES, J. P. F. et al. *S. mansoni-T. cruzi* co-infection modulates arginase-1/iNOS expression, liver and heart disease in mice. **Nitric Oxide.,** v. 66, p. 43-52, 2017.

ROFFÊ, E. *et al.* IL-10 limits parasite burden and protects against fatal myocarditis in a mouse model of *Trypanosoma cruzi* infection. **J Immunol.,** v. 188, n. 2, p. 649-660, 2012.

RONCO, M. T. *et al.* Benznidazole treatment attenuates liver NF-κB activity and MAPK in a cecal ligation and puncture model of sepsis. **Mol Immunol.,** v. 48, n. 6-7, p. 867-873, 2011.

SÁNCHEZ-VILLAMIL, J. P. *et al.* Potential role of antioxidants as adjunctive therapy in chagas disease. **Oxid Med Cell Longev.,** v. 2020, 2020.

SANTOS, E. C. *et al.* Concomitant benznidazole and suramin chemotherapy in mice infected with a virulent strain of *Trypanosoma cruzi*. **Antimicrob Agents Chemother.,** v. 59, n. 10, p. 5999-6006, 2015.

SANTOS, E. C. *et al.* Modulation of oxidative and inflammatory cardiac response by nonselective 1- and 2-cyclooxygenase inhibitor and benznidazole in mice. **J Pharm Pharmacol.,** v. 67, n. 11, p. 1556-1566, 2015.

SANTOS, E. G. *et al.* Could pre-infection exercise training improve the efficacy of specific antiparasitic chemotherapy for Chagas disease? **Parasitology.,** v. 46, n. 13, p. 1655-1664, 2019.

SEQUETTO, P. L. *et al.* Naringin accelerates the regression of pre-neoplastic lesions and the colorectal structural reorganization in a murine model of chemical carcinogenesis. **Food Chem Toxicol.,** v. 64, p. 200-209, 2014.

STORDEUR, P. *et al.* Cytokine mRNA quantification by real-time PCR. **J Immunol Methods.,** v. 259, n. 1-2, p 55-64, 2002.

SUÁREZ, C. *et al.* Diagnosis and clinical management of Chagas disease: An increasing challenge in non-endemic areas. **Res Rep Trop Med.,** v. 13, p. 25-40, 2022.

TIEGHI, T. M. *et al.* Evaluation of antioxidant therapy in experimental Chagas disease. **Rev Soc Bras Med Trop.,** v. 50, n. 2, p. 184-193, 2017.

TORRICO, F. *et al.* New regimens of benznidazole monotherapy and in combination with fosravuconazole for treatment of Chagas disease (BENDITA): a phase 2, double-blind, randomised trial. **Lancet Infect Dis.,** v. 21, n. 8, p. 1129-1140, 2021.

VERCESI, A. E.; FOCESI, A. Effect of 2,4-dinitrophenol on the glycogen phosphorolysis and glycogenolysis in cardiac muscle *in vivo* and *in vitro*. **Rev Bras Pesqui Med Biol.** v. 6, n. 5, p. 235-239, 1973.

VILAR-PEREIRA, G. *et al.* Resveratrol reverses functional chagas heart disease in mice. **PLoS Pathog.,** v. 12, n. 10, 2016.

VILAS-BOAS, D. F. *et al.* 4-nitrobenzoylcoumarin potentiates the antiparasitic, anti-inflammatory and cardioprotective effects of benznidazole in a murine model of acute *Trypanosoma cruzi* infection. **Acta Trop.,** v. 228, 2022.

WEN, J. J.; GARG, N. Oxidative modification of mitochondrial respiratory complexes in response to the stress of *Trypanosoma cruzi* infection. **Free Radic Biol Med.,** v. 37, n. 12, p. 2072-2081, 2004.

WEN, J. J.; GARG, N. J. Mitochondrial generation of reactive oxygen species is enhanced at the Q(o) site of the complex III in the myocardium of *Trypanosoma cruzi*-infected mice: beneficial effects of an antioxidant. **J Bioenerg Biomembr.,** v. 40, n. 6, p. 587-598, 2008.

WORLD HEALTH ORGANIZATION. **Chagas disease (American trypanosomiasis)**. Genebra, Suíça: WHO, 2023. Disponível em: https://www.who.int/news-room/fact-sheets/detail/chagas-disease-(american-trypanosomiasi. Acesso em: 03 jan. 2024.

ZACKS, M. A. *et al.* An overview of chagasic cardiomyopathy: pathogenic importance of oxidative stress. **An Acad Bras Cienc.,** v. 77, n. 4, p. 695-715, 2005.

ZANLUQUI, N. G.; WOWK, P. F.; PINGE-FILHO, P. Macrophage polarization in Chagas disease. **J Clin Cell Immunol.,** v. 6, p. 317, 2015.